MODELLING OF STRESS GRADIENT EFFECT ON FATIGUE LIFE USING WEIBULL BASED DISTRIBUTION FUNCTION

Aleksander Karolczuk, Thierry Palin-Luc

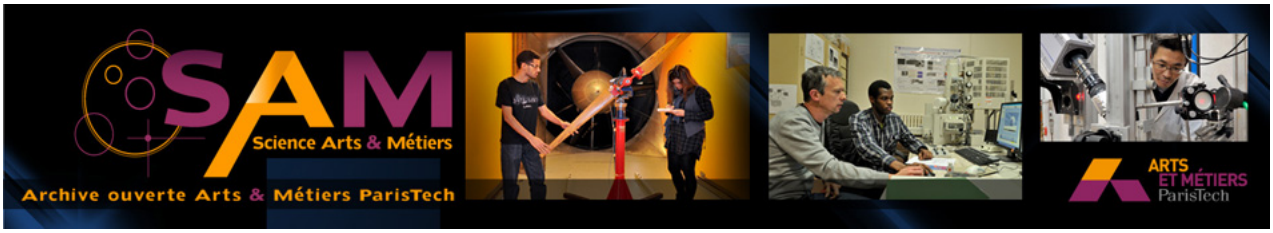

JOURNAL OF THEORETICAL AND APPLIED MECHANICS
51, 2, pp. 297-311, Warsaw 2013

MODELLING OF STRESS GRADIENT EFFECT ON FATIGUE LIFE USING WEIBULL BASED DISTRIBUTION FUNCTION

Aleksander Karolczuk
Opole University of Technology, Department of Mechanics and Machine Design, Opole, Poland
e-mail: a.karolczuk@po.opole.pl

Thierry Palin-Luc
Université Bordeaux 1, Arts et Métiers ParisTech, I2M, UMR CNRS 5295, Talence Cedex, France
e-mail: thierry.palin-luc@ensam.eu

In the present paper, a new approach is developed in order to take into account the stress gradient effect on fatigue life of structural components. The proposed approach is based on the weakest link concept in which the shape coefficient of the Weibull distribution becomes a function of a local damage parameter. The function simulates the experimentally observed relationship between the shape of the fatigue life distribution and the stress level. Such an approach allows one to calculate the global probability distribution of the fatigue life for notched structural components in a wide range of fatigue life regime: 10^4-10^7 cycles typically. For comparison purposes, the approach is applied to calculate the number of cycles to crack initiation of structural elements under three probability levels: 5%, 63% and 95%. The calculated lifetimes are compared with the lifetimes obtained from experiments performed on notched cruciform specimens and notched round specimens subjected to constant amplitude loading.

Key words: fatigue life, stress gradient effect, weakest link concept

Nomenclature

HCF	–	High Cycle Fatigue (HCF, more than $\sim 10^6$ cycles)
LCF	–	Low Cycle Fatigue (LCF, less than $\sim 10^4$ cycles)
MCF	–	Middle Cycle Fatigue (MCF, $\sim 10^4$ to $\sim 10^6$ cycles)
N, N_{exp}	–	fatigue life in cycles and experimental number of cycles to failure
P_f	–	failure probability
$P_s, P_s^{(i)}$	–	survival probability and survival probability of i-th link
t	–	time
ε_n, σ_n	–	normal strain and normal stress (to the critical plane)
Ω_0	–	reference domain
σ_a, σ_{eq}	–	stress amplitude and equivalent stress
σ_{af}	–	classical fatigue limit
σ_{kl}	–	stress tensor components $(k, l = x, y, z)$
σ_0, σ_u, m	–	Weibull parameters: stress shift (or threshold stress), stress scale and shape parameter, respectively

1. Introduction

Effect of fluctuating stresses on fatigue life of structural elements is commonly combined with the effect of heterogeneous stress distribution (stress gradient) because of notches or both complex geometry and loadings. These two factors lead to complex mechanisms of fatigue failure. Two of

them should be clearly distinguished. The first mechanism concerns the case when a particular fatigue crack, responsible for final macroscopic failure of a component, reaches its critical length under the influence of a heterogeneous stress field. The methods that take into account this mechanism are based on averaged stresses (strains) over a material domain. The considered domains could be a volume (Banvillet *et al.*, 2003; Morel and Palin-Luc, 2002), a plane (Morel and Palin-Luc, 2002; Seweryn and Mróz, 1998; Karolczuk, 2008) or their simplifications such as a line domain (Qylafku *et al.*, 1998) or a point domain (Taylor, 1999). The second mechanism is related to a defect distribution or rather to inhomogeneity of the material structure (Morel and Huyen, 2008) and concerns the case when the fatigue failure could start at any elementary domain within the element but the probability of such an event depends on the stress history. Thus, the fatigue failure of the element is a function of both the cyclic stress volumetric distribution and the size of the considered structural element. This mechanism is usually taken into account by probabilistic methods based on the weakest link concept.

The weakest link concept has been used by many researchers (Bomas *et al.*, 1997, 1999; Delahay and Palin-Luc, 2006; Flaceliere and Morel, 2004; Wormsen *et al.*, 2007) to assess the probability distribution of the fatigue limit $(P_f - \sigma_{af})$ for elements in which the stress field is inhomogeneous.

Why these models are not used to calculate the probability distribution of the fatigue life $(P_f - N_f)$*?* There is one main reason. The weakest link concept assumes independence of failure of each link (elementary material domain dA or dV), and it is usually taken for granted that the material is loaded in its pure elastic domain (at the macroscopic scale). Thus, according to many researchers, only the probability distribution of the fatigue limits (no plastic strains) could be determined using the weakest link concept. According to some researchers (Miller and O'Donnel, 1999; Sonsino, 2007; Bathias and Paris, 2005), a real fatigue limit does not exist. Consequently, to be more precise only the fatigue strength distribution at a large number of loading cycles, e.g. $N \approx 5 \cdot 10^6$ or more, could be determined using the weakest link concept. The assumption of a pure elastic material in the case of the component with an inhomogeneous stress field even for a fatigue life close to $N \approx 5 \cdot 10^6$ cycles is doubtful. In Karolczuk (2008), it is shown that macroscopic plastic strains appear within a component under a heterogeneous stress field at a high number of cycles (at the classical fatigue limit). The existing probability models based on the weakest link concept assume a pure elastic state of the material. This is considered to be true under fatigue loading leading to failure around $N_0 = 5 \cdot 10^6$ cycles, and this allows one to calculate the fatigue strength distribution (or the classical fatigue limit).

Why does the existence of macroscopic plastic strains exclude the application of the weakest link concept? At the low loading level (without macroscopic plastic strains), the cracks nucleate in the weakest places within the element (e.g. at the largest defects $\rightarrow$ largest microscopic stress concentration). The lower loading level, the lower the number of nucleated cracks is observed (Morel and Huyen, 2008). According to the weakest link concept, the appearance of the first microcrack defines the failure of the whole element. However, the microcrack has a physical length that is not infinitively small as it is assumed by the weakest link concept. The microcrack must grow to the size that defines the technical failure of the component (or specimen). Usually, a few millimeters. The total fatigue life of the component includes periods of different damage mechanisms. The application of the weakest link concept is fully justified in the regimes where only local damage mechanisms take place. When the local damage mechanism changes to crack growth, the weakest link concept is not applicable. Practically, the failure of a component is usually defined by the critical crack length; but if the crack growth period is short enough compared with the total fatigue life, then the weakest link concept could be applied and could give good results. Higher fatigue loading could create larger plastic strains and a larger number of nucleated microcracks that grow and link together up to the critical crack length is obtained. The larger macroscopic plastic strains make the mesoscopic stress distribution more

uniform which results in a less scattered fatigue life at higher loading, then it is at lower loading (Bastenaire, 1972; Han *et al.*, 1996; Schijve, 1994, 2005; Zheng *et al.*, 1995, 1996). The larger number of microcracks as a result of macroscopic plastic strains convinced many researchers of the inapplicability of the weakest link concept in the LCF regime. However, appropriate failure detection such as a short crack in length that presents prevailing initiation phase could justify the assumption of a dominating period of the local damage mechanisms. Consequently, in such a case, the application of the weakest link concept up to crack initiation should be possible.

Nevertheless, it must be remembered that plastic strains change the probability distribution of the fatigue life. Thus, for a correct calculation of the final (global) fatigue life distribution of a component that includes elementary domains (links) loaded by different stress histories (different plastic strain amplitudes), it is necessary to know the correct fatigue life distribution for each link. The coefficients of these distributions must be a function of the local damage parameters, e.g. stress amplitudes.

The main aim of this paper is to present a method and its algorithm to simulate the fatigue life probability distribution $(P_f - \sigma_a - N)$ of a structural component under a heterogeneous cyclic stress field. In other words, the probabilistic Wöhler curve of a component can be computed with the proposed method. The calculation is performed in a wide range of fatigue life (LCF-HCF), this is possible because the shape of the fatigue life distribution is modeled with regard to a local damage parameter such as the equivalent stress (strain) amplitude. The scale and shape coefficients of the Weibull distribution become functions of equivalent stress (strain) amplitudes. This allows us to simulate the evolution of the scatter band both of the fatigue life and the fatigue strength from LCF to HCF. The proposed functions are simple and are identified using experimental data.

2. Weakest link concept

Foundations of the weakest link concept, being the base of the Weibull theory, were formulated in the twenties of the 20th century. The main assumptions of the weakest link concept are the following: (i) a structure is seen as a series of small elements linked together which include statistically distributed defects; (ii) failure is supposed to occur in a certain elementary area (link) that contains the "most harmful defect" (in fatigue, and according to the authors, failure is seen as crack initiation - technical detectable crack, around 0.2 mm long for the experiments described in Section 5); (iii) the probabilities of failure in each link are independent.

From experiments, it appears that for identical elements (at the macroscopic scale) loaded by time dependent forces $F(t)$, the logarithm of the number of cycles N to crack initiation is a random variable with a given probability density distribution p_f. In a set of successive specimens, "the most harmful defect" exhibits different features, and thus crack initiation occurs under a different number of cycles N. In the case of a heterogeneous stress field, the given specimen is divided into subdomains (links). The probability that a crack will not occur within the life time interval $[0, N]$ means that crack initiation will not occur in any elementary subdomain (weakest link concept). Indicating that $P_s^{(i)}$ is the survival probability means that no crack will initiate in the sub-domain (i) within the number of cycles interval $[0, N]$. Then the survival probability P_s for the whole specimen (or component) is the product of all the individual probabilities $P_s^{(i)}$ because no interaction between defects is assumed, as follows

$$P_s = \prod_{i=1}^{i=k} P_s^{(i)} \tag{2.1}$$

where k is the total number of sub-domains (links). Assuming an exponential form of survival probability $P_s^{(i)} = \mathrm{e}^{-f(\sigma)}$ leads to substitution of product $\prod$ in Eq. (2.1) by summation (in-

tegration) function $P_s = P_s^{(i)} P_s^{(i+1)} \ldots = \mathrm{e}^{-f(\sigma^{(i)})} \mathrm{e}^{-f(\sigma^{(i+1)})} \ldots = \mathrm{e}^{-f(\sigma^{(i)})-f(\sigma^{(i+1)})} \ldots$. Weibull (1939) proposed such a form of survival probability distribution. The classical (Weibull) form of failure probability $P_f = 1 - P_s$ is as follows

$$P_f = 1 - \exp\left(- \frac{1}{\Omega_0} \int\limits_{\Omega} g(\sigma)\, d\Omega \right) \tag{2.2}$$

where

$$g(\sigma) = \left(\frac{\sigma}{\sigma_u} \right)^m \qquad \text{or} \qquad g(\sigma) = \left(\frac{\langle \sigma - \sigma_0 \rangle}{\sigma_u} \right)^m \tag{2.3}$$

Ω_0 is the volume or surface of the reference domain; $g(\sigma)$ is a function called by Weibull "risk of rupture". Its form depends on the material properties, $\langle x \rangle = x$ if $x > 0$ and $\langle x \rangle = 0$ if $x \leqslant 0$. Weibull proposed two forms of the function $g(\sigma)$: with two (Eq. $(2.3)_1$) or three (Eq. $(2.3)_2$) parameters, where σ_0, σ_u, m are parameters called the stress shift (or threshold stress), stress scale and shape parameters, respectively. Owing to different material properties on the surface and in volume due to manufacturing process (for instance), Weibull considered individual failure probability for the volume V ($\Omega = V$) and the surface A ($\Omega = A$). In the case of fatigue processes in a uniaxial loaded component with an homogenous stress distribution with an amplitude σ_a, the failure probability is a two dimensional function of both the stress amplitude σ_a and the fatigue life N, $P_f = F(\sigma_a, N)$. In other words, the fatigue life scatter is obtained under the same stress amplitude σ_a or the same fatigue life may be achieved under different stresses σ_a. Such a two-dimensional function was considered by Weibull (1949), however the mathematical expression was not proposed. When the failure of the element is assigned to a specific fatigue life N, then the failure probability P_f is reduced to the stress function only. This concept is very popular to determine the fatigue limit (Bomas *et al.*, 1997, 1999; Delahay and Palin-Luc, 2006; Flaceliere and Morel, 2004; Wormsen *et al.*, 2007) of the element under a heterogeneous stress distribution. In such a case, the specific fatigue life N is assigned to the lifetime (usually around $10^6 - 5 \cdot 10^6$ cycles) which defines the beginning of the HCF fatigue regime and the "infinite fatigue life" within an engineering point of view.

3. The proposed P-S-N curve model

3.1. Hypothesis

The method proposed hereafter is thought to be implemented under a wide range of the fatigue life regime (i.e. from LCF to HCF, at least from MCF to HCF), it means even if there are macroscopic cyclic plastic strains. Existence of such plastic strains may be considered not in agreement with the Weibull (1939) statement expressed by Eq. (2.2). Indeed, the weakest link concept has been proposed for isotropic brittle-like materials. However, it must be remembered that this equation was proposed to describe the probability distribution of the ultimate tensile strength for which the failure means total fracture (in two parts) of a structural component under quasi-static monotonic tension. This kind of failure is obtained for a brittle-like material just (or quickly) after the failure of one link (elementary sub-domain). Thus, in such a case, the hypothesis of failure independence of each link (sub-domain of the structural element) used to establish Eq. (2.1) and Eq. (2.2) is satisfied. In the case of fatigue loading in the fatigue life regime higher than 10^4 cycles, the hypothesis of failure independence of each sub-domain is restricted. In fact, the problem concerns the material failure definition (see explanation given in Introduction). The most popular definition of the fatigue failure is crack length dependent. The crack length defining the fatigue failure must be obtained in a period dominated by crack

initiation mechanisms (local damage mechanisms) to justify the application of the hypothesis of failure independence of each link. The existence of plastic strains changes the mechanisms of damage, which is seen macroscopically by the change in the distribution shape of the fatigue life. A structural element under an inhomogeneous stress field includes areas under different stress – strain time histories, different macroscopic plastic strains and, consequently, different distribution shapes of the local fatigue lives. These local fatigue lives must be simulated and taken into account for a proper determination of the global probability distribution of the fatigue life of the structural element.

The conclusion is that the weakest link concept might be applied in the fatigue life regime higher than 10^4 cycles if: (i) the appropriate crack length (a physically short crack) defining the failure as a crack initiation is clearly specified, and (ii) the shape change of the fatigue life distribution depending on stress histories in each link is taken into account.

3.2. P-S-N curve model

Different stress courses within a structural element result in an inhomogeneous fatigue damage field. For each point of the considered element, a local damage parameter $\omega(d\Omega)$ may be computed, e.g. an equivalent stress amplitude. The local value of the damage parameter is assumed to be linked with the local probability distribution of the fatigue life, $P_f(N, d\Omega)$. As mentioned in the previous sections, the higher local damage parameter $\omega(d\Omega)$, the lower scatter of the fatigue life. This relation must be well captured by the P-S-N curve model. If the model does not simulate the relationship between the local probability distribution of the fatigue life and the local value of the damage parameter, then the global probability distribution $P_f(N, \Omega)$ obtained by using the weakest link concept is not correct. The originality of the proposed model consists in simulating the local probability distribution of the fatigue life depending on the local value of a damage parameter that allows us to compute the global fatigue life of a structural element for any probability level.

The general form of the probability distribution is analogous to Weibull expression, Eq. (2.2). However, the former stress function of the "risk of rupture" $g(\sigma)$ becomes also function of lifetime N, and the failure probability takes the general form as follows

$$P_f(N, \omega, \Omega) = 1 - \exp\left(- \frac{1}{\Omega_0} \int_{\Omega} h(N, \omega)\, d\Omega \right) \tag{3.1}$$

The failure probability P_f increases with the increasing damage parameter ω but P_f (for a given ω) also increases with the number of cycles N. The longer structural element is in service, the failure probability is higher. Schijve (1993) leans towards a view that the Weibull distribution describes well the scatter of the fatigue life (under a given stress amplitude σ_a) in the logarithmic scale. It could be expressed by the following equation

$$P_f = 1 - \exp\left(- \left(\frac{\log N}{\mu} \right)^m \right) \tag{3.2}$$

where μ is the lifetime scale parameter and m is the shape parameter. Because the magnitude of the fatigue life scatter depends on the damage parameter (stress or strain amplitude), the distribution parameters μ and m must be functions of the damage parameter. In a natural way, the scale parameter μ takes the form $\mu = \log N_f$, where N_f is the characteristic fatigue life (reference) for the probability value $P_f = 1 - \mathrm{e}^{-1} \approx 0.63$. The value of N_f is determined from the reference fatigue curve $\omega - N_f$ (e.g. $\sigma_a - N_f$, if the damage parameter is the stress amplitude). For a given damage parameter, such as the stress amplitude σ_a, the parameter m simulates the shape of distribution that is for the fatigue life scatter. The shape parameter must reflect the relation between the scatter band of the fatigue lives and the value of the damage parameter ω.

Under loading equal to the ultimate quasi-static tensile strength, the fatigue life does not exhibit any scatter compared with the fatigue scatter (in the fatigue sense, N_f tends to a quater of the loading cycle). On the other hand, under loading at the fatigue limit, some specimens fail, and some others have an unlimited fatigue life (if the concept of the fatigue limit is assumed). It means that the scatter of fatigue lives depends on the value of the damage parameter which could be related to $\log N_f$. This relationship is modelled by the following proposed function

$$m(\omega) = m(N_f) = \frac{p}{\log N_f} \tag{3.3}$$

where p is a constant parameter. The mathematical relationship between ω and N_f is known by the empirical reference curves (the Basquin equation for instance). In other words, the coefficient p can be seen as a quality factor of both the manufacturing process of the element and the material (internal defects for instance). Finally, the failure probability distribution of the component takes the form

$$P_f = 1 - \exp\left(- \frac{1}{\Omega_0} \int_{\Omega} \left(\frac{\log N}{\log N_f} \right)^{\frac{p}{\log N_f}} d\Omega \right) \tag{3.4}$$

where $\Omega = V$ or $\Omega = A$. In the case of a uniform distribution of the damage parameter ω over the Ω_0, Eq. (3.4) reduces to

$$P_f = 1 - \exp\left(- \left(\frac{\log N}{\log N_f} \right)^{\frac{p}{\log N_f}} \right) \tag{3.5}$$

For instance, Fig. 1a shows an example of two-dimensional failure probability distribution according to Eq. (3.5), using the fatigue reference curve $(\omega - N_f)$. Figure 1b illustrates the reference curve $\omega - N_f$ along with the scatter band for $P_f = 0.05$ and $P_f = 0.95$ is shown.

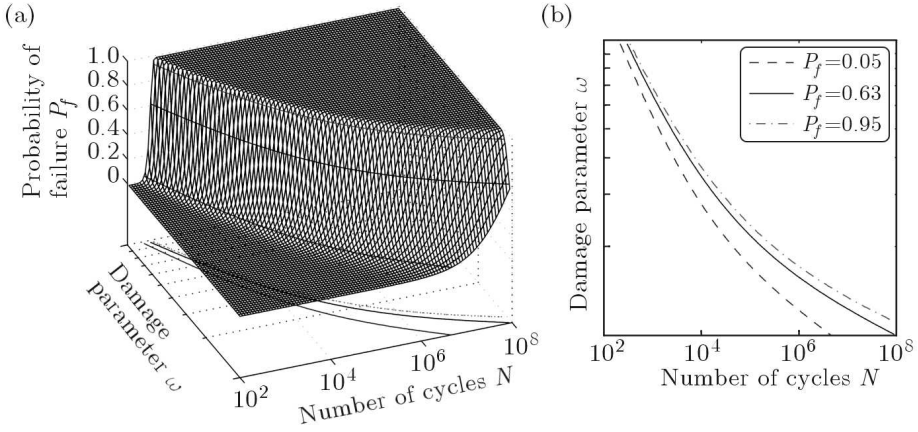

Fig. 1. (a) Simulated two-dimensional distribution of the failure probability P_f; (b) fatigue reference curve $\omega - N_f$ with the fatigue scatter bands for $P_f = 0.05$ and $P_f = 0.95$

Crossing the two-dimensional distribution $P_f(\omega, N)$ by a horizontal plane $P_f = \text{const}$, the fatigue reference curve $\omega - N$ for $P_f = \text{const}$ is obtained. An important point is to realize that the conventional reference curve $\sigma_a - N_f$ obtained from experimental fatigue tests with the least square method corresponds to $P_f \approx 0.63$, if the experimental fatigue data (N_{exp}, σ_a) follow the probability distribution expressed by Eq. (3.5), Fig. 1. This result comes from the exponential form of the survival probability. This is discussed below.

The fatigue limit σ_{af} is usually determined from experimental results by applying the staircase procedure that defines the median fatigue limit (it means for a failure probability of 0.5).

This value is used in many probabilistic methods (Bomas *et al.*, 1997, 1999; Delahay and Palin-Luc, 2006; Flaceliere and Morel, 2004; Wormsen *et al.*, 2007) that are focused on the fatigue limit assessment. However, it must be noted that the conventional reference fatigue curve is identified from experimental points (N_{exp}, σ_a) by the least square method (ASTM E739-91, 1998) which unnecessary leads to results so that 50% of the experimental points (N_{exp}, σ_a) are on the left side of the reference curve and 50% of the experimental points are on the right side. This feature comes from the minimization of summed distances between the experimental fatigue lives $N_{exp}^{(j)}$ and the evaluated ones from the reference curve lives $N_f^{(j)}$, $\min \sum_{j=1}^{M} (N_f^{(j)} - N_{exp}^{(j)})^2$ (M is the total number of specimens used to identify the reference curve, j is the subsequent index). Applying failure probability distribution Eq. (3.5) to the reference specimens, i.e. $N = N_f$ shows that the reference fatigue curve $(\sigma_a - N_f)$ corresponds to a probability equal to $P_f = 1 - \mathrm{e}^{-1} \approx 0.63$.

4. Implementation of the two-dimensional probability distribution P_f for fatigue life calculations

4.1. FEA and the proposed model

Let us assume that the cracks occurring on the free surface of the considered structural element are responsible for failure ($\Omega = A$ and $\Omega_0 = A_0$ in Eq. (3.4)). If the parameters of two-dimensional probability distribution (3.4) are known, the procedure of the fatigue life assessment for a structural element with a heterogeneous stress distribution is as follows:

- The free surface of the considered element is divided into sub-domains $A^{(i)}$; their sizes allow an appropriate integration process (Fig. 2a)
- In each sub-domain $A^{(i)}$, any multiaxial stress state $\sigma_{kl}^{(i)}(t)$ (where k, l are tensor indexes) is reduced to an equivalent stress amplitude $\sigma_{eqa}^{(i)}$ (where *eqa* means the equivalent amplitude) by using a multiaxial fatigue crack initiation criterion
- The equivalent stress amplitude $\sigma_{eqa}^{(i)}$ and the fatigue reference curve $\sigma_a - N_f$ are used for calculating the scale parameter $\log N_f^{(i)}$ for each sub-domain $A^{(i)}$ (Fig. 2b). Then, the survival probability distribution $P_s^{(i)}$ is determined (Fig. 2b) as follows

$$P_s^{(i)}(N) = \exp\left(-\frac{1}{A_0} \left(\frac{\log N}{\log N_f^{(i)}} \right)^{\frac{p}{\log N_f^{(i)}}} A^{(i)} \right) \tag{4.1}$$

- For each fatigue life N, exponents of e natural logarithm are summed over all the sub-domains A(i) and the survival probability distribution Ps(N) (Fig. 2c) for the whole structural element is obtained,

$$P_s(N) = \exp\left(-\frac{1}{A_0} \sum_{i=1}^{i=k} \left(\frac{\log N}{\log N_f^{(i)}} \right)^{\frac{p}{\log N_f^{(i)}}} A^{(i)} \right) = \prod_{i=1}^{i=k} P_s^{(i)}(N) \tag{4.2}$$

- The fatigue life calculation N_{cal} is performed for $P_f(N_{cal}) = 0.63$. The fatigue life for any other probability level can be calculated in a similar way.

It has to be noticed that the proposed method can be applied with any equivalent stress assumption (i.e. multiaxial fatigue criterion). The equivalent stress is chosen to transform any multiaxial stress state in a uniaxial one, which is supposed to generate an equivalent fatigue life according to the chosen damage parameter.

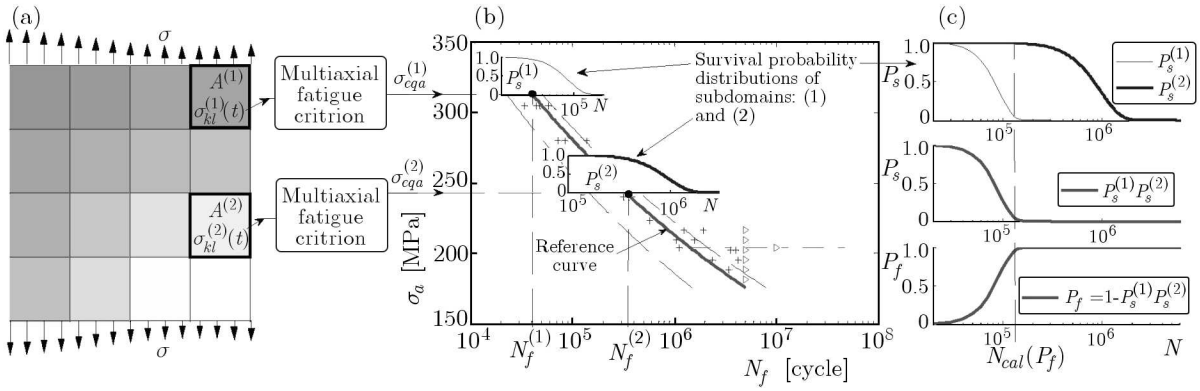

Fig. 2. Scheme of the model: (a) separated sub-domains $A^{(i)}$ of the structural element; (b) distributions of survival probability $P_s^{(i)}(N)$ of particular sub-domains against the fatigue reference curve; (c) individual survival probability distributions $P_s^{(i)}(N)$ in each sub-domain $A^{(i)}$ undergoing into survival probability $P_s(N) = \prod_{i=1}^{i=k} P_s^{(i)}(N)$ of the structural element and failure probability distribution

$$P_f(N) = 1 - \prod_{i=1}^{i=k} P_s^{(i)}(N)$$

4.2. Identification of the parameters

Taking advantage of the empirical analytic equation of the reference Wöhler curve $\sigma_a - N_f$, the two-dimensional distribution given by Eq. (3.4) has only two parameters to be identified, i.e. A_0 and p. The reference surface area A_0 is the free surface area of the specimen applied for determining the reference Wöhler curve.

The parameter p characterizes the distribution of the fatigue life in the model. It can be identified from the fatigue test results of specimens having the similar distribution of defects (kind and morphology) as the considered element. However, the manufacturing qualities of structural elements and specimens are usually different (the surface roughness for instance). In such a case, the distribution parameters should be fitted on the basis of one series of tests carried on a real element subjected to simple fatigue loadings. Such a procedure was used, for example, by Delahay and Palin-Luc (2006) for the identification of the fatigue strength probability distribution parameters. In the present paper, the authors apply different values of the parameter p to find the best correlation between experimental fatigue lives N_{exp} and the calculated fatigue lives N_{cal}. This is also an indirect way to quantify the sensitivity of the proposed model to the value of p.

5. Experimental fatigue tests and results

Experimental results obtained from testing two steels with different specimen geometries were used for analysing and verification of the proposed probabilistic method.

In the first set of experiments, cruciform specimens made of S355 J2G3 steel (Fig. 3 and Table 1) with a central hole as stress concentrator (stress concentration factors in tension K_t approaches to 3) were subjected to a biaxial fatigue loading (Karolczuk *et al.*, 2007).

Cyclic properties of the tested steel, i.e. the relation between the number of cycles to failure N_f and the stress amplitude σ_a (under load control) as well as parameters of the cyclic hardening curve ($\varepsilon_a^p - \sigma_a$ under strain control) are given in Table 1 from tests on smooth specimens. The fatigue tests on notched specimens (Fig. 3) were carried out under force control with: $F_x(t) = F_{xa}\sin(2\pi ft)$, $F_y(t) = F_{ya}\sin(2\pi ft - \delta)$ with the same frequency in each direc-

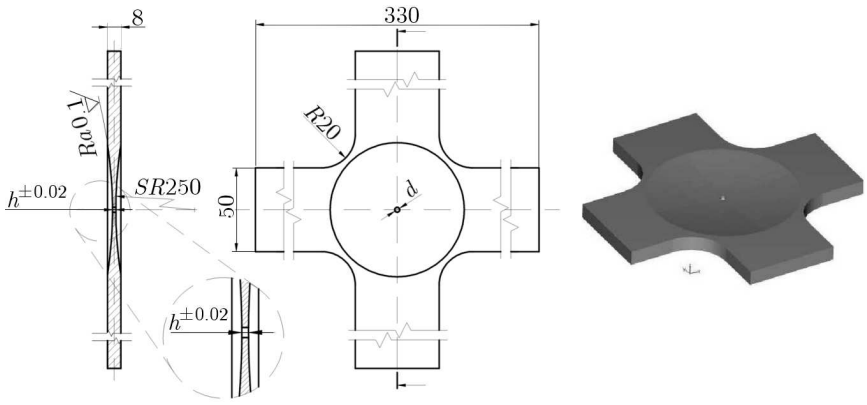

Fig. 3. Geometry of a cruciform specimen made of S355 J2G3 steel

Table 1. Cyclic properties of S355 J2G3 steel under fully reversed tension for smooth specimens

$\sigma_a = \sigma_{af}(N_\sigma/N_f)^{1/m_\sigma}$			$\varepsilon_a^p = (\sigma_a/K')^{1/n'}$		A_0
σ_{af} [GPa]	m_σ	N_σ [cycles]	K' [MPa]	n' [–]	[mm^2]
204	8.32	$1.426 \cdot 10^6$	1323	0.207	1256

Indices: af – fatigue limit at N_σ cycles, a – amplitude, p – plastic part

tion ($f = 13\,\mathrm{Hz}$) and similar amplitudes F_{xa} and F_{ya} with the phase shift $\delta = 180°$ (Table 2). Table 2 contains also the numbers of cycles to crack initiation N_k corresponding to the crack length a_k. The crack length a_k is the length of the first registered crack. The crack lengths were identified from pictures made with an optical microscope (magnification 7×) and a digital camera (0.0085 mm/pixel). The pictures of the specimen surface near the hole were periodically taken in order to detect the number of cycles N_k when the crack initiation occurs and to analyse the crack growth rate. The last photography without the visible crack was taken at N_0 cycles, which shows the measuring accuracy of the crack initiation life N_k (Table 2).

Table 2. Test conditions and results

Specimen	d [mm]	h [mm]	F_{xa} [kN]	F_{ya} [kN]	N_k [cycle]	a_k [mm]	N_0 (no crack) [cycle]
P02	3.0	1.40	13.30	13.10	39700	0.22	22500
P03	3.0	1.54	13.50	13.30	31100	0.37	20100
P04	3.0	1.86	13.55	13.30	60048	0.07	50400
P05	2.5	1.50	10.21	9.90	246695	0.25	225400
P07	3.0	1.75	11.20	10.80	140700	0.20	108200
P08	2.4	1.20	9.30	9.10	167050	0.10	156800

The second set of experimental results comes from the work of Fatemi *et al.* (2004). A circumferentially notched round bar (Fig. 4) made of vanadium-based micro-alloyed forged steel, in both as-forged (AF) and quenched and tempered (QT) conditions were subjected to a fully reversed tension-compression loading. In the as-forged (AF) condition, two notch radii were tested, $R = 0.529\,\mathrm{mm}$ and $R = 1.588\,\mathrm{mm}$ which generate the following stress concentration factors in tension $K_t = 2.8$ and $K_t = 1.8$, respectively. Under the quenched and tempered (QT) condition, only one specimen geometry with the notch radius $R = 1.588\,\mathrm{mm}$ ($K_t = 1.8$) was tested. The parameters of the reference Manson-Coffin-Basquin curve are presented in Table 3.

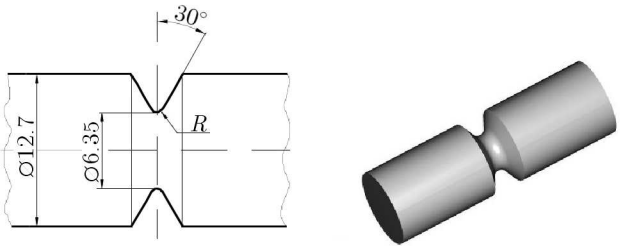

Fig. 4. Geometry of a round notched specimen, where $R = 0.529\,\text{mm}$ ($K_t = 2.8$) or $R = 1.588\,\text{mm}$ ($K_t = 1.8$) (Fatemi *et al.*, 2004)

Table 3. Cyclic properties of AISI 1141 steel in two conditions: as-forged (AF) and quenched and tempered (QT)

$\varepsilon_a = \sigma'_f/E(2N_f)^b + \varepsilon'_f(2N_f)^c$						$\varepsilon_a^p = (\sigma_a/K')^{1/n'}$		A_0
State	E [GPa]	σ'_f [MPa]	ε'_f [–]	b	c	K' [MPa]	n' [–]	[mm^2]
AF	200	1296	1.026	−0.088	−0.686	1205	0.122	162
QT	212	765	1.664	−0.041	−0.704	1133	0.134	162

The fatigue life of the notched and smooth (reference) specimens were defined as the number of cycles endured until the specimen broke in two parts. However, Fatemi *et al.* (2004) observations carried out with a travelling microscope (with 30× magnification) show that macro-crack growth life was not a significant part of the total life (Fatemi *et al.*, 2004). Therefore, the number of cycles up to crack initiation could be assumed equal to the total fatigue life.

6. Numerical simulations and results

The strain and stress distribution in the specimens were calculated using a 3D finite element analysis with COMSOL software. In all the computations, a cyclic constitutive model with linear kinematic hardening was applied. The material hardening was identified from the cyclic hardening curve (from half-life hysteresis loops) expressed by the Ramberg-Osgood $\varepsilon_a^p = (\sigma_a/K')^{1/n'}$ equation. The plasticity condition was defined by the conventional Huber-Mises-Hencky hypothesis. Quadratic Lagrange elements (tetrahedrons order 2) with higher mesh density in the vicinity of the notch were used in the computations. Because of both the symmetry of the loading and the geometry of the specimens, only 1/8 part of the cruciform specimens was modelled, and 1/32 part of round notched specimen was modelled. A detailed analysis of the mesh size influence on the fatigue life calculation has been performed. A different maximum size of the finite element (MES) in the notch surface of the cruciform specimen (P02 in Table 2) has been analysed. The results are shown in Table 4. The computed fatigue lives do not vary significantly (up to 7.9%). To save computation time for further computation of other cruciform, specimens MES = 0.15 mm have been selected. Similar analysis has been performed for the round specimen whose results were obtained with MES = 0.10 mm for $R = 0.529\,\text{mm}$ ($K_t = 2.8$) and MES = 0.20 mm for $R = 1.588\,\text{mm}$ ($K_t = 1.8$).

The reference curves (amplitudes of normal stress or strain versus lifetime) were obtained under a simple loading condition, i.e. push-pull, which has generated a uniaxial stress state in the smooth-reference specimens. The same kind of loading was applied to notched specimens where the notch generated a multiaxial stress state. Because in both cases (i.e. the smooth reference and notched specimens) the loadings were similar, the multiaxial stress/strain state at every point in specimen volume was reduced to normal stress/strain as used in the reference curves.

Table 4. Effect of maximum element size on stress and fatigue life calculation (for $p = 580$ and $P_f = 0.63$)

Max Element Size (MES) [mm]	$\max_i A^{(i)}$ [mm^2]	Solution time [s]	N_{cal} ($P_f = 0.63$) [cycle]	$N_{cal}/43030$
0.10	0.0056	542	43030	1.000
0.15	0.0134	304	43337	1.007
0.25	0.0264	204	41565	0.966
0.30	0.0309	204	43734	1.016
0.40	0.0670	184	46418	1.079

Indeed, fatigue tests on theses specimens showed that the fracture plane was also perpendicular to the maximum principal stress. Thus, the fatigue criterion of the maximum normal stresses (cruciform specimens) or strains (round specimen) on the critical plane was assumed to be the criterion of multiaxial fatigue crack initiation (Karolczuk and Macha, 2005).

The equivalent stresses or strains are calculated according to the following equations

$$\begin{aligned} \sigma_{eq}(t) &= \sigma_n(t) = \sigma_{ij}(t) n_i n_j \\ \varepsilon_{eq}(t) &= \varepsilon_n(t) = \varepsilon_{ij}(t) n_i n_j \end{aligned} \tag{6.1}$$

where n_i are the components of the unit normal vector to the plane experiencing the maximum normal stress $\max\limits_{t,\mathbf{n}} \sigma_n(t)$ or strain $\max\limits_{t,\mathbf{n}} \varepsilon_n(t)$. Under the considered cyclic reversal loadings, the equivalent stress/strain amplitude Eq. (6.1) at each point on the notch surface is equal to the maximum principal stress/strain in the considered loading period. Owing to that, numerical calculations become easier. Surfaces of the finite elements were understood as sub-domains $A^{(i)}$ described in Section 2. Fatigue lives to crack initiation N_{cal} were calculated for three failure probability levels: $P_f = \{0.05; 0.63; 0.95\}$ and for different values of the p parameter (Figs. 5 and 6). The upper $P_f = 0.95$ and lower $P_f = 0.05$ bands of failure probability are marked by plus (+) in Figs. 5 and 6. The fatigue life attained for the failure probability $P_f = 0.63$ is indicated by a filled black circle (•). Two additional scatter bands ($\times 2$ and $\times 3$) around the solid line for the perfect result ($N_{cal} = N_{exp}$) consistency are also shown in Fig. 5a. For AISI 1141 steel in both condition (AF) and (QT), the best agreement between the calculated and experimental fatigue lives was obtained for $p = 340$ (Fig. 6b). It must be noted that independently on the notch radius R (Fig. 5) and specimen state (AF) or (QT), the best agreement between N_{exp} and N_{cal} was obtained for only one value of p ($p = 340$). Since the surface qualities of specimens are similar in these cases, the obtained results are in agreement with the assumption that the p coefficient is a manufacturing quality dependant factor. For S355 J2G3 steel, the best fatigue lives correlation was attained for $p = 580$, see Fig. 5. A comparison Fig. 5a and Fig. 5b shows the influence of parameter p on the calculated fatigue life and on the fatigue life range included between $P_f = 0.05$ and $P_f = 0.95$. A greater value of p leads to a higher calculated fatigue life $N_{cal}(P_f = 0.63)$ and a lower calculated scatter band $N_{cal}(P_f = 0.95)/N_{cal}(P_f = 0.05)$.

The results presented in Fig. 7 concerning S355 J2G3 steel subjected to push-pull loading (the reference curve) show that for a large range of fatigue life the experimental points $\sigma_a - N_f$ are included in the scatter band defined by $P_f = \{0.05; 0.95\}$. Only for $N_f > N_\sigma = 1.24 \cdot 10^6$ cycles ($N\sigma$ corresponding to the experimental fatigue limit) the fatigue life scatters are greater than the defined band because the applied reference curve is not able to capture asymptotic nature of S-N curve tendency when N tends to infinity.

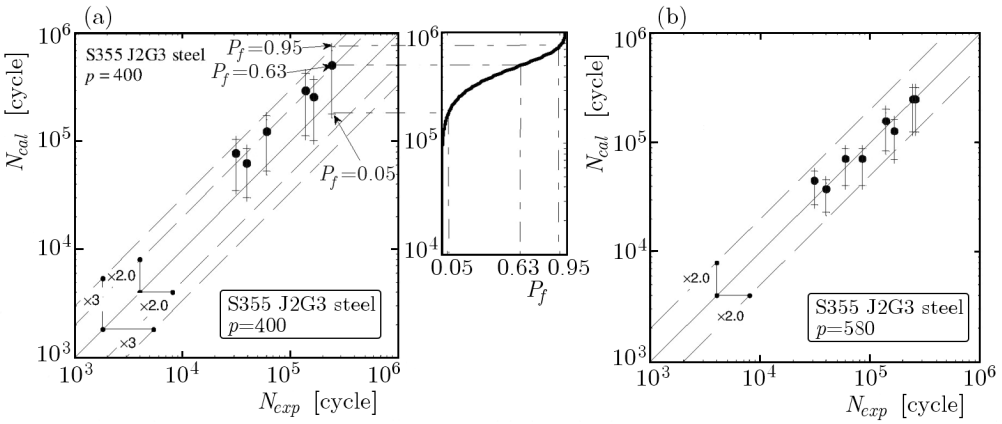

Fig. 5. Comparison of the experimental fatigue lives N_{exp} with the calculated lives N_{cal} for (a) $p = 400$ and (b) $p = 580$ for the cruciform specimens in S355 J2G3 steel under out of phase ($-180°$) biaxial tension

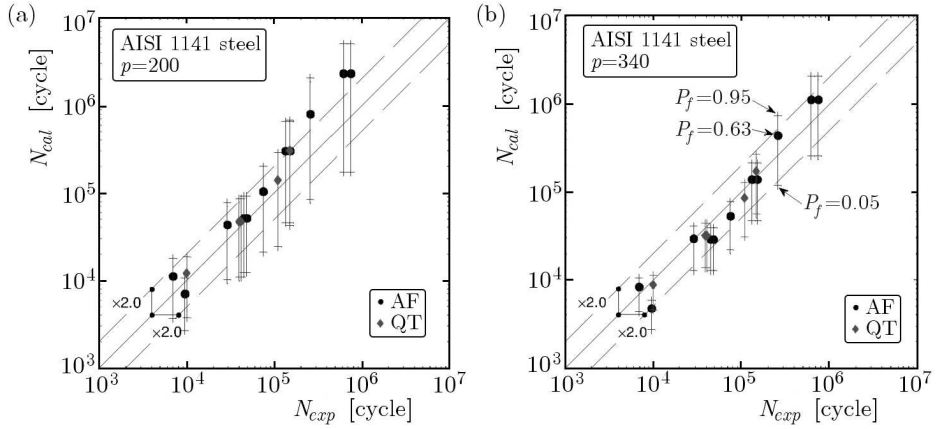

Fig. 6. Comparison of the experimental lives N_{exp} with the calculated lives N_{cal} for (a) $p = 200$ and (b) $p = 340$ for the notched round specimens in AISI 1141 steel under fully reversed tension

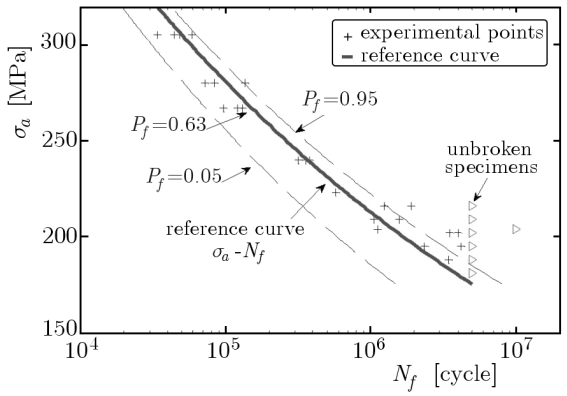

Fig. 7. Fatigue reference curve $\sigma_a - N_f$ (S355 J2G3 steel) with experimental points and fatigue scatter bands for $P_f = 0.05$ and $P_f = 0.95$ ($p = 580$)

7. Conclusions

The weakest link concept has been applied to simulate both the fatigue life and the failure probability of structural elements under an inhomogeneous cyclic stress field. In the proposed model, the shape of the probability distribution of the fatigue life for each link of the structural

element is a function of the local damage parameters such as the equivalent stress or strain amplitude. The introduced relation simulates the experimentally observed relationship between the distribution shape of the fatigue life and the loading level. Proposed function (3.3) relates the scale and shape coefficients of the Weibull distribution.

The presented probability distribution Eq. (3.4) has a general form. It can be used with different fatigue damage parameters (stress, strain or energy) and also under a variable amplitude loading.

The calculated fatigue lives N_{cal} for failure probability equal to 63% are well correlated with the experimental fatigue lives N_{exp} for notched round specimens made of AISI 1141 steel (with $p = 340$) independently of the notch radius and material state (QT or AF) and for the notched cruciform specimens made of S355 J2G3 steel (with $p = 580$).

To compute the proposed probability distribution function given by (3.4) of the fatigue life, the identification of only one additional parameter p is needed. This parameter can be seen as a quality factor of both the element manufacturing process and the material (internal defects, size and morphology for instance). Such a simple form is suitable for the considered two types of notched specimens. However, it should be expected that other elements made of the same steels but with different qualities (manufacturing process, surface roughness, etc.) would reveal other values of the parameter p.

References

1. ASTM E739-91, 1998, *Standard Practices for Statistical Analysis of Linear or Linearized Stress-Life (S-N) and Strain-Life* ($\varepsilon - N$) *Fatigue Data*, ASTM International, West Conshohocken, PA, www.astm.org
2. Banvillet A., Łagoda T., Macha E., Niesłony A., Palin-Luc T., Vittori J.-F., 2004, Fatigue life under non-Gaussian random loading from various models, *Int. J. Fatigue*, **26**, 349-363
3. Banvillet A., Palin-Luc T., Lasserre S., 2003, A volumetric energy based high cycle multiaxial fatigue criterion, *Int. J. Fatigue*, **25**, 755-769
4. Bastenaire F.A., 1972, New method for the statistical evaluation of constant stress amplitude fatigue-test results. Probabilistic aspects of fatigue, *ASTM STP*, **511**, 3-28
5. Bathias C. and Paris P.C., 2005, *Gigacycle Fatigue in Mechanical Practice* Marcel Dekker Editions, New York
6. Bomas H., Mayr P., Schleicher M., 1997, Calculation method for the fatigue limit of parts of case hardened steels, *Materials Science and Engineering*, **A234-236**, 393-396
7. Bomas H., Linkewitz T. Mayra P., 1999, Application of a weakest-link concept to the fatigue limit of the bearing steel SAE 52100 in a bainitic condition, *Fatigue Fract. Engng Mater. Struct.*, **22**, 733-741
8. Bomas H., Mayr P. Linkewitz T., 1999, Inclusion size distribution and endurance limit of a hard steel, *Extremes*, **2**, 2, 149-164
9. Carpinteri A., Spagnoli A., Vantadori S., 2003, A multiaxial fatigue criterion for random loading, *Fatigue Fract. Engng Mater. Struct.*, **26**, 515-522
10. COMSOL, 2006, Structural Mechanics Module User's Guide, version 3.3
11. Dang Van K., 1983, Macro-micro approach in high-cycle multiaxial fatigue, [In:] *Advances in Multiaxial Fatigue*, McDowell D.L. and Ellis R. (Edit.), American Society for Testing and Materials STP 1191, 120-130
12. Dang Van K., Cailletaud G., Flavenot J.F., Le Douaron A., Lieurade H.P., 1989, Criterion for high cycle fatigue failure under multiaxial loading, [In:] *Biaxial and Multiaxial Fatigue* Brown M. and Miller K.J. (Edit.), Mechanical Engineering Publications, 459-478

13. Delahay T., Palin-Luc T., 2006, Estimation of the fatigue strength distribution in high-cycle multiaxial fatigue taking into account the stress–strain gradient effect, *Int. J. Fatigue*, **28**, 474-484

14. Fatemi A., Zeng Z., Plaseied A., 2004, Fatigue behavior and life predictions of notched specimens made of QT and forged microalloyed steels, *Int. J. Fatigue*, **26**, 663-672

15. Flaceliere L., Morel F., 2004, Probabilistic approach in high-cycle multiaxial fatigue: volume and surface effects, *Fatigue Fract. Engng Mater. Struct.*, **27**, 1123-1135

16. Han F., Billardon R., Beranger A.S., 1996, Fatigue failures maps of heterogeneous materials, *Mechanics of Materials*, **22**, 11-21

17. Karolczuk A, Macha E., 2005, A review of critical plane orientations in multiaxial fatigue failure criteria of metallic materials, *Int. J. Fract.*, **134**, 267-304

18. Karolczuk A., Lachowicz C.T., Rozumek D. Słowik J., 2007, Inicjacja i rozwój pęknięć zmęczeniowych w próbkach krzyżowych z karbem, *Przegląd Mechaniczny*, **12**, 7, 18-23 [In Polish]

19. Karolczuk A., 2008,. Non-local area approach for fatigue life evaluation under combined reversed bending and torsion, *Int. J. Fatigue*, **30**, 1985-1996

20. Miller K.J., O'Donnell W.J., 1999, The fatigue limit and its elimination, *Fatigue Fract. Engng Mater. Struct.*, **22**, 545-557

21. Morel F., Huyen N., 2008, Plasticity and damage heterogeneity in fatigue, *Theoretical and Applied Fracture Mechanics*, **49**, 98-127

22. Morel F. and Palin-Luc T., 2002,. A non local theory applied to high cycle multiaxial fatigue, *Fatigue Fract. Engng Mater. Struct.*, **25**, 649-665

23. Murakami Y., Endo M., 1994, Effect of defect, inclusions and inhomogeneities on fatigue strength, *Int. J. Fatigue*, **16**, 163-182

24. Papadopoulos I.V., Panoskaltsis V.P., 1996, Invariant formulation of a gradient dependent multiaxial high-cycle fatigue criterion, *Engng Fract. Mech.*, **55**, 4, 513-528

25. Papadopoulos I.V., Davoli P., Gorla C., Filippini M., Bernasconi A., 1997, A comparative study of multiaxial high-cycle fatigue criteria for metals, *Int. J. Fatigue*, **19**, 3, 219-235

26. Papadopoulos I.V., 2001, Long life fatigue under multiaxial loading, *Int. J. Fatigue*, **23**, 831-849

27. Qylafku G., Azari Z., Gjonaj M, Pluvinage G., 1998, On the fatigue failure and life prediction for notched specimens, *Materials Science*, **34**, 5, 604-618

28. Schijve J., 1993, A normal distribution or a Weibull distribution for fatigue lives, *Fatigue Fract. Engng Mater. Struct.*, **16**, 8, 851-859

29. Schijve J., 1994, Fatigue predictions and scatter, *Fatigue Fract. Engng Mater. Struct.*, **17**, 381-396

30. Schijve J., 2005, Statistical distribution functions and fatigue of structures, *Int. J. Fatigue*, **27**, 1031-1039

31. Seweryn A., Mróz Z., 1998, On the criterion of damage evolution for variable multiaxial stress states, *Int. J. Solids Structures*, **35**, 14, 1589-1616

32. Sonsino C.M., 2007, Course of SN-curves especially in the high-cycle fatigue regime with regard to component design and safety, *Int. J. Fatigue*, **29**, 2246-2258

33. Taylor D., 1999, Geometrical effects in fatigue: a unifying theoretical model, *Int. J. Fatigue*, **21**, 413-420

34. Weibull W., 1939, A statistical theory of the strength of materials, *Royal Swed. Inst. Engng Res.*, **151**, Sweden

35. Weibull W., 1949, A statistical representation of fatigue failures in solids, *Transaction of the Royal Institute of Technology*, **27**, Sweden

36. Wormsen A., Sjödin B., Hrkegrd G. Fjeldstad A., 2007, Non-local stress approach for fatigue assessment based on weakest-link theory and statistics of extremes, *Fatigue Fract. Engng Mater. Struct.*, **30**, 1214-1227

37. Zheng X., Lü B., Jiang H., 1995, Determination of probability distribution of fatigue strength and expressions of P-S-N curves, *Engng Fract. Mech.*, **50**, 4, 483-491

38. Zheng X., Li Z., Lü B., 1996, Prediction of probability distribution of fatigue life of 15MnVN steel notched elements under variable-amplitude loading, *Int. J. Fatigue*, **18**, 2, 81-86

Modelowanie efektu gradient naprężeń na trwałość zmęczeniową przy zastosowaniu funkcji bazującej na rozkładzie Weibulla

Streszczenie

W artykule zaprezentowano nową koncepcję uwzględnienia wpływu gradientu naprężeń na trwałość zmęczeniową elementów konstrukcyjnych. Przedstawione podejście bazuje na koncepcji najsłabszego ogniwa, w której współczynnik kształtu rozkładu Weibulla jest funkcją lokalnego parametru uszkodzenia. Zaproponowana funkcja symuluje obserwowany eksperymentalnie związek między kształtem rozkładu trwałości zmęczeniowej a amplitudą naprężenia. Podejście takie umożliwia wyznaczenie globalnego rozkładu prawdopodobieństwa zniszczenia dla elementów z karbem w szerokim zakresie trwałości: 10^4-10^7 cykli. Dla celów porównawczych zaproponowane podejście zostało zastosowane do obliczenia liczby cykli do inicjacji pęknięcia dla trzech poziomów prawdopodobieństwa, tj. 5%, 63% oraz 95%. Obliczone trwałości zmęczeniowe zostały porównane z trwałością eksperymentalną otrzymaną dla próbek krzyżowych z karbem oraz dla próbek cylindrycznych z karbem obrączkowym.

Manuscript received April 20, 2012; accepted for print June 14, 2012